

Original

Yi, S.; Bohlen, J.; Sandloebes, S.; Zaefferer, S.; Letzig, D.; Kainer, K.U.:
**Microstructural evolution during recrystallization of
magnesium alloys**
Materials Science Forum, THERMEC 2011 (2012)
Trans Tech Publications

DOI: [10.4028/www.scientific.net/MSF.706-709.1291](https://doi.org/10.4028/www.scientific.net/MSF.706-709.1291)

MICROSTRUCTURAL EVOLUTION DURING RECRYSTALLIZATION OF MAGNESIUM ALLOYS

Sangbong Yi^{1, a}, Jan Bohlen^{1, b}, Stefanie Sandlöbes^{2, c}, Stefan Zaefferer^{2, d},
Dietmar Letzig^{1, e} and Karl Ulrich Kainer^{1, f}

¹MagIC-Magnesium Innovation Centre, Helmholtz-Zentrum Geesthacht, Max-Planck-Str. 1, 21502, Geesthacht, Germany

²Max-Planck-Institute for Iron Research, Max-Planck-Str. 1, 40237, Düsseldorf, Germany

^asangbong.yi@hzg.de, ^bjan.bohlen@hzg.de, ^cs.sandloebes@mpie.de, ^ds.zaefferer@mpie.de,
^edietmar.letzig@hzg.de, ^fkarl.kainer@hzg.de

Keywords: Magnesium, Recrystallization, Grain growth, Texture, Shear bands

Abstract. Microstructural evolution during the annealing of cold rolled Mg, Mg-1.5Nd and Mg-3Y sheets has been examined. The experimental results show a significant difference in recrystallization kinetics and grain growth between pure Mg and Mg-RE alloy sheets. Pure Mg sheet shows rapid recrystallization and grain growth, whereas recrystallization is considerably retarded in the Mg-RE alloys. Although recrystallized grains which are triggered at shear bands in the cold rolled pure Mg sheet show a relatively weak texture with a basal pole split into the sheet rolling direction, rapid grain growth is accompanied by re-strengthening of the basal-type texture. In contrast, a weak texture appears in the early recrystallization stage in Mg-RE alloys and is retained during annealing due to retarded recrystallization and grain growth.

Introduction

The industrial application of Mg alloy sheets is hindered by their poor formability and strong mechanical anisotropy. In general a strong basal-type texture which causes poor formability is formed in Mg alloys by thermo-mechanical treatments. These grain orientations are unfavourable for basal $\langle a \rangle$ dislocation slip, which is the easiest deformation mode in Mg alloys, under loading along the sheet planar and normal directions (ND). Therefore, texture modification to give a broadening or weakening of the basal pole has been suggested as an effective way of improving sheet formability. A number of studies have shown that alloying additions of rare-earth (RE) elements to Mg alloys result in a significant weakening of the basal-type texture [1-3]. Among the different mechanisms proposed to explain the formation of more random textures in Mg-RE alloys, changes in deformation mechanisms and recrystallization kinetics are favoured to explain this observation. A recent study clarified the mechanisms responsible for changes in the deformation texture in Mg-RE alloys [4]. Rolled sheets of Mg-RE alloys show a large number of contraction-, secondary twins as well as high activity of $\langle c+a \rangle$ pyramidal slip, processes which are seldom observed in pure Mg and conventional Mg alloys, such as the AZ alloys. Although various mechanisms of texture weakening in Mg-RE alloys during recrystallization have been suggested by different research groups, e.g. particle stimulated nucleation [5], shear band nucleation [6, 7] and restricted grain boundary mobility [2] due to Zener-Smith or solute drag, it is still a matter of discussion which of these mechanisms plays a major role and how the different mechanisms interact.

The present study examines the evolution of microstructure and texture during annealing of cold rolled Mg alloy sheets experimentally. By comparative studies of pure Mg, Mg-1.5Nd and Mg-3Y (in wt. %) alloy sheets, the role of the RE addition on the microstructural evolution has been investigated. To minimize the effect of dynamic recrystallization on the final microstructure, cold rolling was employed as the deformation process. However, it is important to mention that the ratio between the room temperature and the melting temperature of pure Mg is about 1/3 (in K) so that DRX can occur during deformation of pure Mg at room temperature.

Experimental procedures

Mg-1.5Nd and Mg-3Y (in wt.%) alloys were cast into steel moulds using an electrical furnace under Ar + SF₆ atmosphere, while a commercially available cast block served as an initial material for pure Mg. Slabs were machined from the cast blocks with a thickness of 25 mm and a width of 50 mm. After hot rolling at 450 °C to a thickness of 2 mm, the plates were further cold rolled at room temperature to 1 mm which corresponds to 50 % thickness reduction. To avoid cracking during cold rolling, the thickness reduction per pass was controlled so as not to exceed 4 %, as suggested in the literature [8, 9]. Figure 1 presents the surface appearance of the cold rolled sheets after 50 % thickness reduction. Only a small amount of edge cracks with lengths of 2 ~ 3 mm appear after cold rolling to 50 % thickness reduction even in pure Mg, so that microstructural studies at the mid part of the sheets were not influenced by cracking. The cold rolled sheets were annealed at 350°C for different times, from 5 to 3600 s, under atmospheric conditions.

The microstructure and texture of the rolled and annealed sheets were investigated using electron backscatter diffraction (EBSD) and X-ray diffraction. For X-ray diffraction, 6 incomplete pole figures of {10-10}, (0002), {10-11}, {10-12}, {11-20} and {10-13} planes were collected, and the complete pole figures were calculated using MTEX software [10]. EBSD measurements were conducted on the longitudinal sections parallel to the RD. Samples were prepared by mechanical polishing using alumina powder followed by electrolytic polishing using a Struers AC2 solution (for 90 s at 33 V and -25°C).

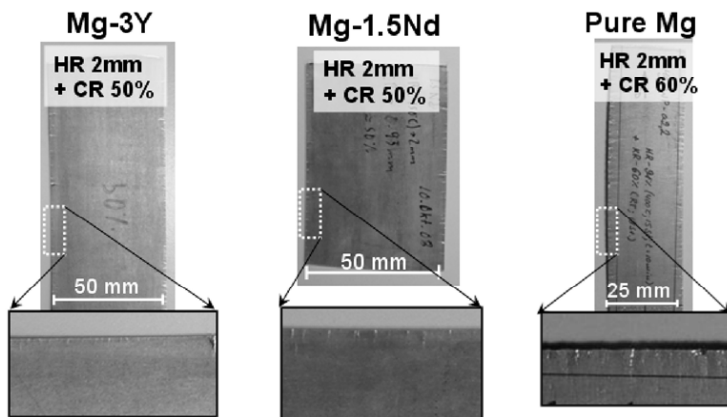


Fig. 1. Surface appearance of the cold rolled Mg-3Y (50 % thickness reduction), Mg-1.5Nd (50 %) and pure Mg (60 %) sheets.

Results and discussion

Optical micrographs of RD-ND sections and recalculated (0002) pole figures from XRD measurements of the hot rolled sheets as well as those sheets that were subsequently cold rolled are

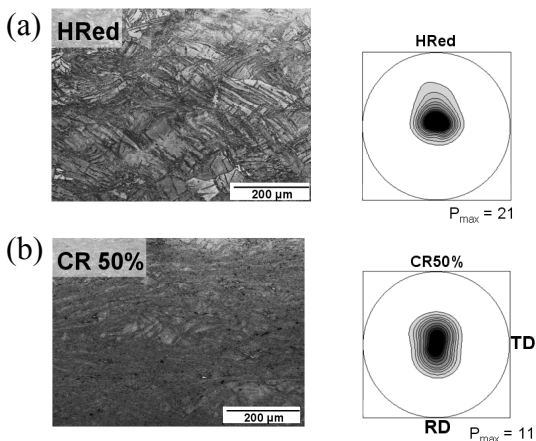


Fig. 2. Optical micrographs and recalculated (0002) pole figures of (a) hot rolled to 2 mm and (b) 50 % cold rolled to 1 mm pure Mg sheet. Contour levels = 1, 1.5, 2, 2.5, 3, 4, 5, 6, 7 mrd (multiple random degree).

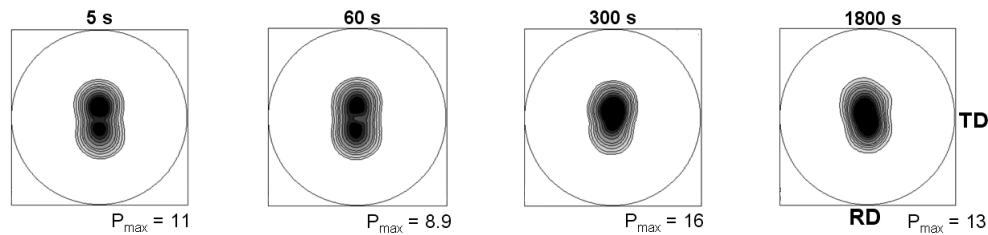


Fig. 3. Recalculated (0002) pole figures after annealing of the 50 % cold rolled pure Mg sheets at 350 °C for various times; 5 s, 60 s, 300 s and 1800 s.

shown in Figure 2 for pure magnesium. A highly deformed microstructure is observed in the hot rolled sheet with a large amount of contraction and secondary twins, which were examined by EBSD measurements (not shown). The activation of $\{10\text{-}11\}$ contraction and $\{10\text{-}11\}$ - $\{10\text{-}12\}$ secondary twins during hot rolling of pure Mg was reported in previous EBSD studies [3, 11]. The coverage of the shear bands becomes gradually larger after cold rolling, such that the sheet shows shear bands developing throughout the whole sheet thickness. Interestingly, the texture intensity in terms of the max (0002) pole density, P_{\max_0002} , decreases after cold rolling, e.g. $P_{\max_0002} = 21$ and 11 m.r.d. in the hot rolled and cold rolled conditions, respectively. The decrease in the texture intensity is associated with the increase of shear band coverage due to cold rolling, because the severe deformation at these localized areas results in more diffuse orientations. It is also apparent that the cold rolling process leads to a slight broadening of the basal poles into the RD. The XRD-textures of the annealed pure Mg sheets for various holding times at 350 °C are illustrated in Figure 3. The sheets annealed for 5 s and 60 s show relatively weak textures, $P_{\max_0002} = 11$ and $P_{\max_0002} = 8.9$, respectively, with a basal pole split of about 15 ° into the RD. Recalling the previous observations of [4, 12, 13] which describe the shear bands as the areas having more random orientations and split basal poles, the appearance of the basal pole split during the early annealing stage in the present study is related to recrystallization within the shear bands. Further annealing leads to the disappearance of the basal pole split and a strengthening of the basal-type texture, as can be seen in the sample annealed for 300 s. It is noteworthy that the decrease in texture sharpness observed after annealing for 1800 s is caused by rapid grain coarsening and, therefore, poor grain statistics for the XRD-texture measurement. The EBSD analysis in Figure 4 shows that the recrystallization process in the cold rolled pure Mg is surprisingly rapid, such that the 5 s annealed sample shows an area fraction of recrystallized grains of 0.64 and a fully recrystallized microstructure is observed after annealing for 60 s. An analysis based on the in-grain misorientation degree was employed to evaluate the area fraction of the recrystallized grains. As the in-grain misorientation degree reflects the density of geometrically necessary dislocations, the grains having an in-grain misorientation degree larger than 1° are supposed to be the deformed ones, whereas

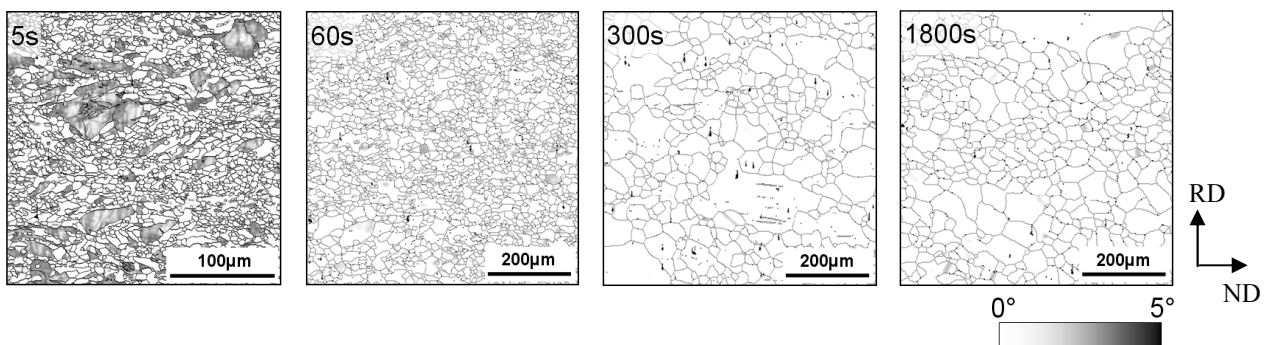


Fig. 4. EBSD local misorientation maps of annealed Mg sheets after various holding times at 350 °C. The color changes correspond to the local orientation deviations from the average orientation within a grain. Because of rapid grain growth, scale bars of different lengths are used.

grains with an in-grain misorientation smaller than 0.5° are supposed to be recrystallized. In the in-grain misorientation maps in Figure 4, the deformed structures can be recognized by the contrast changes (from white to dark grey) and the recrystallized ones by no orientation gradient (no color change within a grain). The recrystallized grains in the sample annealed for 5 s have an average grain size of $7 \pm 2 \mu\text{m}$, whereas the average grain size of the sample annealed for 3600 s is $54 \pm 19 \mu\text{m}$. The above results indicate clearly that rapid grain growth is accompanied by the formation of a strong basal-type texture, while the early recrystallization stage relates to a shear band controlled process resulting in a weak texture with the basal pole tilted towards the RD.

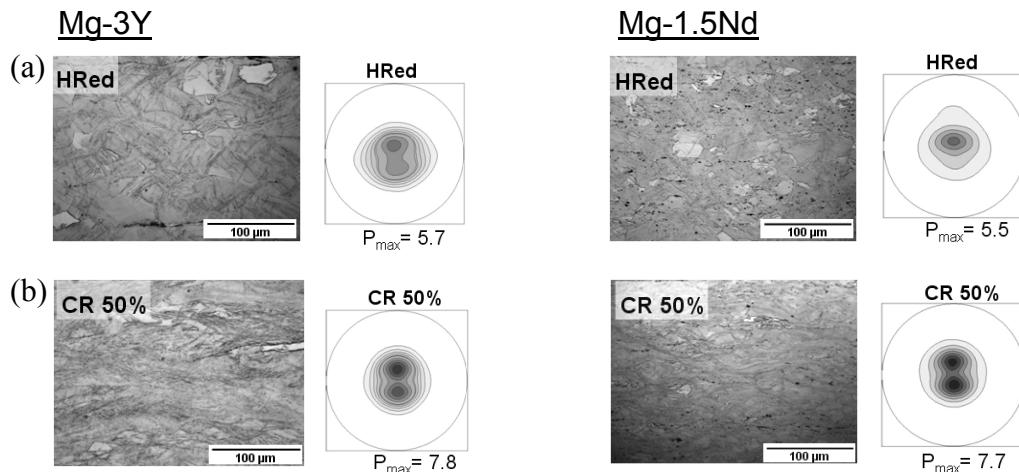


Fig. 5. Optical micrographs and recalculated (0002) pole figures of (a) hot rolled to 2 mm and (b) subsequently 50 % cold rolled to 1 mm Mg-3Y and Mg-1.5Nd sheets. Contour levels = 1, 1.5, 2, 2.5, 3, 4, 5, 6, 7 mrd.

The optical micrographs and XRD-textures of the Mg-3Y and Mg-1.5Nd sheets after hot rolling and after subsequent cold rolling are presented in Figure 5. The microstructures of the hot rolled Mg-RE sheets are similar to those of pure Mg, i.e. highly deformed grains and many twins. However, microstructural evolution during cold rolling of the Mg-RE sheets is different to that observed in the pure Mg sheet. As reported in [4], shear banding in Mg-RE alloys evolves only in some grains, in contrast to the macroscopic shear bands developed throughout the whole sheet thickness in pure Mg. Moreover, the homogeneously distributed band structures initiated from twins in the Mg-RE alloy sheets serve to retard fracture at macroscopic shear bands [4]. Differently to the cold rolled pure Mg sheets, the texture sharpness increases and the split of the basal poles becomes more obvious after cold rolling of the Mg-RE alloy sheets. This indicates in turn that deformation in

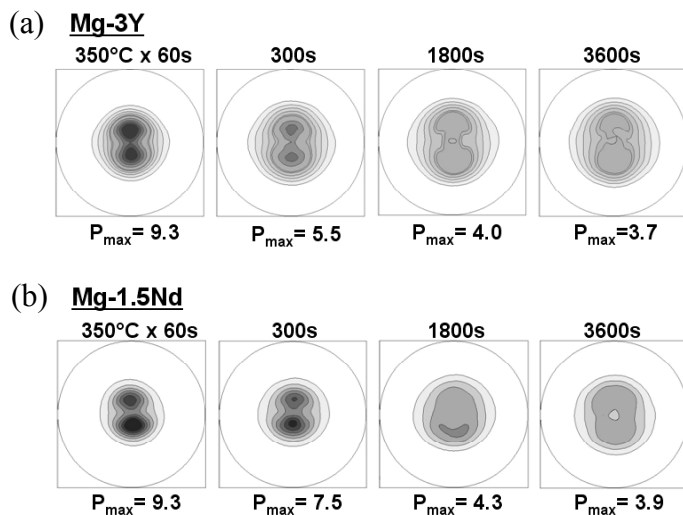
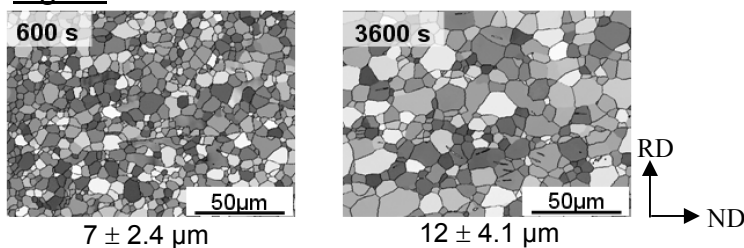


Fig. 6. Recalculated (0002) pole figures after the annealing of the 50 % cold rolled Mg-RE sheets at 350°C for various times, 60 s, 300 s, 1800 s and 3600 s: (a) Mg-3Y and (b) Mg-1.5Nd sheets.

the Mg-RE alloys is accommodated by dislocation slip and twinning, rather than macroscopic shear band formation, which actually leads to texture weakening. This texture evolution with a basal pole split, attributed to the high activity of $\langle c+a \rangle$ slip, was also shown by Agnew et al [14] in a Y containing Mg alloy sheet. The recalculated (0002) pole figures of the cold rolled Mg-RE sheets measured after different holding times at 350 °C are presented in Figure 6. Although the textures of the Mg-RE sheets annealed for 60 s are comparable to that of the pure Mg sheet annealed for 60 s, the subsequent texture evolution is completely different. Both the Mg-3Y and Mg-1.5 sheets show a gradual texture weakening with increasing annealing time. The feature of the split basal pole is kept during annealing up to 3600 s of the Mg-RE alloy sheets, whereas for the pure Mg sheet the split character disappears after annealing for 300 s. In addition, texture weakening is accompanied by an increase in the angular distance between the two maxima in the basal pole figures, from $\sim 30^\circ$ in cold rolled sheet to $\sim 50^\circ$ after annealing for 3600 s.

Mg-3Y



Mg-1.5Nd

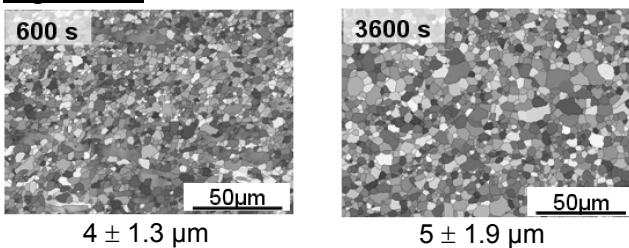


Fig. 7. EBSD inverse pole figure maps in the ND of the cold rolled Mg-3Y (top) and Mg-1.5Nd (bottom) sheets after annealing for 600 s and 3600 s. The average grain size for each annealing condition is also given.

The EBSD inverse pole figure maps of the Mg-RE sheets annealed for 600 s and 3600 s are presented in Figure 7. Unlike the pure Mg sheet, which shows rapid grain growth, the Mg-RE sheets show a fine homogeneous grain structure even after annealing for 3600 s. It should be mentioned that the partially recrystallized microstructures of the Mg-RE alloys after annealing for 180 s are comparable to that of the pure Mg sheet after annealing for 5 s, e.g. the area fraction of recrystallized grains after 180 s annealing = 0.35 and 0.42 for Mg-3Y and Mg-1.5Nd, respectively. The above results indicate clearly that recrystallization and grain growth are significantly retarded in the Mg-3Y and Mg-1.5Nd alloys. The retarded recrystallization process results from the existence of heavy RE atoms in solid solution which hinders grain boundary mobility. Moreover, recrystallization and grain growth are impeded considerably by the existence of Mg-RE precipitates, which is the case for the Mg-1.5Nd alloy examined in the present study. The experimental conditions of the present study, e.g. annealing temperature of 350 °C at which the Mg-1.5Nd alloy is located in the (Mg) + Mg₁₂Nd and / or Mg₄₁Nd₅ two phase region of the binary phase diagram, leads to precipitation during annealing. On the other hand, the annealing temperature of 350 °C corresponds to the (Mg) single phase region for the Mg-3Y alloy. The second phase particles precipitated during the annealing of the Mg-1.5Nd sheet in the present study lead to additional retardation of recrystallization and grain growth by the Zener-Smith drag mechanism, such that a more fine grained structure results in Mg-1.5Nd compared to Mg-3Y sheet.

From the viewpoint of texture development, the retarded grain growth in the Mg-RE alloys has important consequences. Because the rapid growth of grains with a particular orientation, such as the basal-type orientation in pure Mg, is hindered by the pinning effects of the solute atoms and/or precipitates, grains having diverse orientations can grow more equivalently. Consequently, the weak

texture caused by recrystallization at shear bands and the matrix grains deformed more homogeneously via $\langle c+a \rangle$ slip and contraction as well as secondary twins can be retained during grain growth.

Summary

Rapid recrystallization and grain growth occur during the annealing of a cold rolled pure Mg sheet at 350 °C. A relatively weak texture triggered at shear bands disappears with rapid growth of grains having basal-type orientations. In contrast, the recrystallization process is significantly retarded in RE containing Mg alloys by solute and Zener-Smith drag. The retarded recrystallization and grain growth provide an equal growing probability for diversely oriented grains that are nucleated in shear bands as well as in grains deformed more homogeneously by $\langle c+a \rangle$ slip and twins. Therefore, the annealing of Mg-RE alloys results in a gradual texture weakening.

Acknowledgements

It is gratefully acknowledged that the present study is supported by the DFG-German Research Foundation (under grant YI103/1-2 and ZA278/6-2). The authors are grateful to Dr. P. Beaven at the Helmholtz-Zentrum Geesthacht for fruitful discussion and to V. Kree at the Max-Planck-Institute for Iron Research and Y.K. Shin at the HZG for the technical support.

References

- [1] J. Bohlen, M.R. Nürnberg, J.W. Senn, D. Letzig, S.R. Agnew, *Acta Mater.* 55 (2007) 2101.
- [2] L.W.F. Mackenzie, M.O. Pekguleryuz, *Scripta Mater.* 59 (2008) 665.
- [3] K. Hantzsche, J. Bohlen, J. Wendt, K.U. Kainer, S. Yi, D. Letzig, *Scripta Mater.* 63 (2010) 725.
- [4] S. Sandlöbes, S. Zaeferrer, I. Schestakow, S. Yi, R. Gonzalez-Martinez, *Acta Mater.* 59 (2011) 429.
- [5] E.A. Ball, P.B. Pagnell, *Scripta Metall. Mater.* 31 (1994) 111.
- [6] F.J. Humphreys, M. Hatherly, *Recrystallization and Related Annealing Phenomena*, Elsevier Ltd, Oxford, 1996.
- [7] N. Stanford, M.R. Barnett, *Mater. Sci. Eng. A496* (2008) 399.
- [8] J.C. McDonald, *Tans. AIME* 137 (1940) 430.
- [9] S.L. Couling, J.F. Pashak, L. Sturkey, *Trans. ASM* 51 (1958) 94.
- [10] F. Bachmann, R. Hielscher, H. Schaeben, *Solid State Phenomena* 160 (2010) 63.
- [11] S. Yi, I. Schestakow, S. Zaeferrer, *Mater. Sci. Eng. A516* (2009) 58.
- [12] M.R. Barnett, M.D. Nave, C.J. Bettles, *Mater. Sci. Eng. A386* (2004) 205.
- [13] X. Huang, K. Suzuki K, A. Watazu, I. Shigematsu, N. Saito, *J. Alloys Compd.* 457 (2008) 408.
- [14] S.R. Agnew, M.H. Yoo, C.N. Tome, *Acta Mater.* 49 (2001) 4277.